

Silybin, a component of silymarin, exerts anti-inflammatory and anti-fibrogenic effects on human hepatic stellate cells[☆]

Marco Trappoliere¹, Alessandra Caligiuri¹, Monika Schmid¹, Cristiana Bertolani¹, Paola Failli², Francesco Vizzutti¹, Erica Novo³, Carlo di Manzano⁴, Fabio Marra^{1,6}, Carmela Loguercio⁵, Massimo Pinzani^{1,6,*}

¹Dipartimento di Medicina Interna, Università degli Studi di Firenze, Viale G.B. Morgagni, 85, 50134 Florence, Italy

²Dipartimento di Farmacologia Preclinica e Clinica, Università degli Studi di Firenze, Florence, Italy

³Dipartimento di Medicina e Oncologia Sperimentale, Università degli Studi di Torino, Turin, Italy

⁴IBI Istituto Biochimico Italiano Giovanni Lorenzini, Seconda Università di Napoli, Naples, Italy

⁵Dipartimento di Gastroenterologia, Seconda Università di Napoli, Naples, Italy

⁶Center for Research, High Education and Transfer DENOThe, University of Florence, Florence, Italy

Background/Aims: Hepatic fibrogenesis, a consequence of chronic liver tissue damage, is characterized by activation of the hepatic stellate cells (HSC). Silybin has been shown to exert anti-fibrogenic effects in animal models. However, scant information is available on the fine cellular and molecular events responsible for this effect. The aim of this study was to assess the mechanisms regulating the anti-fibrogenic and anti-inflammatory activity of Silybin.

Methods: Experiments were performed on HSC isolated from human liver and activated by culture on plastic.

Results: Silybin was able to inhibit dose-dependently (25–50 μ M) growth factor-induced pro-fibrogenic actions of activated human HSC, including cell proliferation ($P < 0.001$), cell motility ($P < 0.001$), and *de novo* synthesis of extracellular matrix components ($P < 0.05$). Silybin (25–50 μ M), inhibited the IL-1-induced synthesis of MCP-1 ($P < 0.01$) and IL-8 ($P < 0.01$) showing a potent anti-inflammatory activity. Silybin exerts its effects by directly inhibiting the ERK, MEK and Raf phosphorylation, reducing the activation of NHE1 (Na^+/H^+ exchanger, $P < 0.05$) and the I κ B α phosphorylation. In addition, Silybin was confirmed to act as a potent anti-oxidant agent.

Conclusion: The results of the study provide molecular insights into the potential therapeutic action of Silybin in chronic liver disease. This action seems to be mostly related to a marked inhibition of the production of pro-inflammatory cytokines, a clear anti-oxidant effect and a reduction of the direct and indirect pro-fibrogenic potential of HSC.

© 2009 European Association for the Study of the Liver. Published by Elsevier B.V. All rights reserved.

Keywords: Silybin; Hepatic inflammation; Fibrogenesis

Received 25 July 2008; received in revised form 19 December 2008; accepted 4 February 2009; available online 5 April 2009

Associate Editor: A. Geerts[†]

[☆] C.D.M. has declared a relationship with the manufacturers of the drugs involved; all the other authors who have taken part in this study declared that they do not have anything to disclose regarding funding or conflict of interest with respect to the manuscript.

* Corresponding author. Tel.: +39 055 4296473; fax: +39 055 417123.

E-mail address: m.pinzani@dmi.unifi.it (M. Pinzani).

Abbreviations: CLD, chronic liver disease; DMNQ, 2,3-dimethoxy-1-naphthoquinone; ECM, extracellular matrix; HSC, hepatic stellate cells; H₂O₂, hydrogen peroxide; IL, interleukin; [Ca²⁺]_i, intracellular free calcium concentration; [³H]TdR, methyl-[³H] thymidine; MCP-1, monocyte chemoattractant protein-1; PDGF, platelet-derived growth factor; SFIF, serum-free/insulin-free; TGF- β -1, transforming growth factor- β 1; X/XO, xanthine/xanthine oxidase.

1. Introduction

Liver injury and consequent hepatic fibrogenesis may be caused by various agents, including infection with hepatitis viruses, chronic alcohol abuse, metabolic or autoimmune diseases, iron and copper accumulation and parasitic infection. An early event in the development of hepatic fibrosis is the activation of the hepatic stellate cells (HSC), a liver-specific type of pericyte residing in the sub-endothelial space of Disse. Upon activation, resulting from the complex interaction of growth factors, cytokines, oxidative stress and modification of Na^+/H^+ exchange activity, HSC change their phenotype into myofibroblast-like cells with increased production of extracellular matrix (ECM) components such as collagens I and III, proteoglycans, fibronectins, and hyaluronic acid, up-regulation of expression of several plasma membrane receptors such as PDGF-receptors (PDGF-R), acquisition of a contractile apparatus and up-regulation of type I collagen gene [1–4]. Moreover, HSC play an important role in the recruitment of inflammatory cells at sites of liver injury during hepatic inflammation by synthesizing various cytokines and chemokines such as monocyte chemoattractant protein-1 (MCP-1), ICAM-1 and interleukin (IL)-8 [5,6].

At present, no effective anti-fibrogenic therapy is available for the treatment of fibrosis in chronic liver diseases (CLD). The introduction of drugs directly able to reduce the fibrogenic progression, employed in association with clinical strategies directed at reducing the primary cause of liver damage would be an important advancement in the treatment of these disorders.

Silymarin is a flavonoid anti-oxidant isolated from the fruits of milk thistle, *Silybum marianum*. This extract contains well-defined ingredients. Among these, the polyphenole Silybin, a flavolignane representing approximately 60% of Silymarin, has been identified as the major active moiety and has been proposed as an anti-hepatotoxic agent for the treatment of various liver diseases [7–9]. In addition, several recent studies have shown the potential cancer preventive and therapeutic efficacy of Silybin in different animal models and cell culture systems [10,11]. These positive effects have been ascribed to the putative anti-oxidant, anti-inflammatory and anti-proliferative properties of Silybin based on the modulation of specific signalling pathway, transcription factor and gene expression [12,13]. Recently, Polyak et al. have shown, in an *in vitro* system, the anti-inflammatory and anti-HCV effects of a standardized Silymarin extract [14], suggesting a complementary and alternative therapy in patients with chronic hepatitis C infection. In addition, a possible direct effect on HCV replication has been preliminarily suggested in non-responder patients with chronic HCV infection [15].

The anti-fibrotic efficacy of Silymarin and Silybin is primarily supported by results obtained in animal models of

chronic liver disease [16–18]. In these studies, Silybin significantly inhibited liver fibrosis. This effect was associated with a reduction of alpha-smooth muscle positive cells and pro-collagen mRNA. In addition, one study has shown an inhibitory effect of Silymarin on basal cell proliferation in rat HSC [19]. No information is available however concerning the cellular and molecular mechanisms responsible for these effects, particularly in human HSC.

Aim of this study was to assess the potential role of Silybin in modulating the pro-fibrogenic and pro-inflammatory activity of human HSC, the main cellular effectors of hepatic fibrosis, and to understand molecular and cellular mechanisms responsible for these effects.

2. Materials and methods

2.1. Reagents

Phosphorylation-specific antibodies against ERK, Akt, Raf, MEK, I κ B α were purchased from Cell Signalling Technology (Beverly, MA). Monoclonal antibodies against β -actin were purchased from Sigma (St. Louis, MO). Human recombinant PDGF-BB and human recombinant IL-1 β were purchased from Peprotech (Rock Hill, NJ). Methyl-[3H] thymidine ([3H]TdR) was from New England Nuclear (Milan, Italy). Silybin was purchased from INDENA (Milano, Italy).

2.2. Isolation and culture of human hepatic stellate cells

Human HSC were isolated from wedge sections of normal human liver unsuitable for transplantation, as previously reported [20,21]. Briefly, after digestion with collagenase/pronase, HSC were separated from other liver non-parenchymal cells by ultracentrifugation over gradients of Stractan (Cellsep isotonic solution; Larex Inc., St. Paul, MN). Characterization was performed as described elsewhere [20]. Cells were cultured on plastic culture dishes in Iscove's modified Dulbecco's medium supplemented with 0.6 U/mL of insulin, 2.0 mmol/L of glutamine, 0.1 mmol/L of nonessential amino acids, 1.0 mmol/L of sodium pyruvate, antibiotic-antimycotic solution (all provided by Gibco Laboratories, Grand Island, NY), and 20% fetal bovine serum (Imperial Laboratories, Andover, UK). Experiments described in this study were performed on cells between the first and third serial passages (1:3 split ratio) by employing three independent cell preparations. At these stages of culture, human HSC showed transmission electron microscopy features of myofibroblast-like cells, thus indicating complete transition to their activated phenotype.

2.3. DNA synthesis

DNA synthesis was measured as the amount of [3H]TdR incorporated into trichloroacetic acid – precipitable material, as described elsewhere [22]. Briefly, 90% confluent cells were incubated in serum-free/insulin-free (SFIF) medium for 48 h and stimulated for 20 h with PDGF-BB (10 ng/mL) in the presence or absence of Silybin. After 4 h of pulsing with 1.0 $\mu\text{Ci}/\text{mL}$ of [^3H]TdR, cells were washed and lysed, and the amount of [^3H]TdR incorporated was measured. Results were expressed as counts per minute per 10^5 cells.

2.4. Cell growth assay

A total of 10^4 HSC were plated in 12-well dishes and incubated in SFIF for 24 h. Cells were then stimulated with PDGF-BB (10 ng/mL) in the presence or absence of Silybin (5–50 μM) (time 0) for different time periods and counted. Cell counts were performed on triplicate wells on day 0 and after 2, 4, and 6 days. Fresh medium and agonists were added to the remaining wells at each time point.

2.5. Chemotactic assay

Cell migration was performed as previously described [23]. Briefly, modified Boyden chambers equipped with 8- μ m-porosity polyvinylpyrrolidone-free polycarbonate filters were used after pre-coating (20 μ g/mL of human type I collagen; 30 min at 37 °C). Confluent HSC were incubated in SFIF medium for 48 h and then treated with the compound to be tested. After trypsinization, 4×10^4 cells were added to the top chamber and incubated at 37 °C for 6 h. The lower chamber was filled with SFIF medium (control) or PDGF-BB (10 ng/mL) in the presence or absence of Silybin used in the pre-incubation period. Filters were fixed with 96% methanol and stained with Harris' hematoxylin, mounted, and viewed at 450 \times magnification. Migrated cells were quantified as the means \pm SD in 10 randomly chosen high-power fields.

2.6. Wound-healing assay

For the measurement of cell migration during wound healing, human HSC were seeded on 6-well plates coated with type I collagen (20 μ g/mL) and grown to confluence in Iscove's medium containing 20% fetal bovine serum. Confluent cell cultures were incubated in SFIF medium for 48 h before the beginning of the experiment. Monolayers were then disrupted to generate a linear wound of approximately 1 mm with a cell scraper, washed to remove debris, and incubated in medium containing PDGF-BB (10 ng/mL) in the presence or absence of increasing doses of Silybin for 20 h. Cells were subsequently fixed and observed by phase contrast microscopy. Experiments were performed in duplicate, and two fields of each well were recorded.

2.7. Analysis of cytotoxicity

Confluent HSC were incubated in SFIF medium for 24 h and exposed to increasing concentrations of Silybin. Cell viability was evaluated by the trypan blue dye exclusion test at the end of a 24 to 48-h incubation period.

2.8. Detection of intracellular levels of ROS

HSC were seeded in 12-well culture plates (10⁵ cells/well) and then exposed to hydrogen peroxide (H₂O₂) 50 μ M, xanthine/xanthine oxidase (X/XO) (0.2 mM–20 mU) or 2,3-dimethoxy-1-naphthoquinone (DMNQ) 0.1 μ M for 15 min. Intracellular generation of ROS was detected by using the conversion of 2',7'-dichlorodihydrofluorescein diacetate (DCFH-DA, used at 5 μ M concentration), once taken up by cells and de-acetylated by esterase, into the corresponding fluorescent derivative [24]. Cells were observed and photographed under a Zeiss fluorescence microscope.

2.9. Western blot analysis

HSC were harvested, washed with cold PBS [10 mmol/L (pH 7.4)] and lysed in RIPA buffer [20 mmol/L Tris-HCl, pH 7.4, 150 mmol/L NaCl, 5 mmol/L ethylenediaminetetraacetic acid, 1% Nonidet P-40, 1 mmol/L Na₃VO₄, 1 mmol/L phenyl methyl sulfonyl fluoride, and 0.05% (w/v) aprotinin] for 30 min. The cell lysate was centrifuged at 12,000 r/min for 10 min and the supernatant was collected for Western blot analysis. Protein concentration was measured in triplicate using a commercially available assay (BCATM Protein Assay Kit, Pierce, Rockford, IL). Protein samples were subjected to 10% SDS-PAGE gel electrophoresis and then transferred into a nitrocellulose membrane by electro-blotting. Membranes were stained with 0.5% Ponceau and blocked for 1 h with 5% milk in PBS- 0.1% Tween 20. Afterward, membranes were incubated with the primary antibody followed by the secondary antibody, horseradish peroxidase-conjugated goat anti-rabbit IgG antibody (Santa Cruz Biotechnology, Santa Cruz, CA), incubated for 1 h at room temperature.

Immunodetected proteins were visualized using ECL assay kit (Amersham Biosciences).

2.10. Intracellular calcium concentration

Digital video imaging of the intracellular free calcium concentration ([Ca²⁺]_i) in individual human HSC was performed as described [25]. Subconfluent HSC were grown in complete medium on glass cover slips and then incubated for 48 hours in SFIF medium. Cells were then loaded with 4 μ mol/L of Fura-2-AM and 15% Pluronic F-127 (both obtained by Molecular Probes) for 45 min at 22 °C. [Ca²⁺]_i was measured in Fura-2-loaded cells in HEPES/NaHCO₃ buffer containing 140 mmol/L of NaCl, 3 mmol/L of KCl, 0.5 mmol/L of NaH₂PO₄, 12 mmol/L of NaHCO₃, 1.2 mmol/L of MgCl₂, 1.0 mmol/L of CaCl₂, 10 mmol/L of HEPES, and 10 mmol/L of glucose (pH 7.4). Ratio images (340–380 nm) were collected every 3 s. PDGF-BB (10 ng/ml) was added directly to the perfusion chamber after the [Ca²⁺]_i basal value was recorded. Cells were pre-incubated with Silybin 10 min before stimulation.

2.11. Measurement of Na⁺/H⁺ antiporter activity

Human HSC (grown on glass coverslips until 70% confluence and maintained for 48 h in SFIF) were loaded with 2 μ mol/L of bis-carboxyethylcarboxyfluorescein (BCECF) for 30 min at room temperature and washed. Fluorescence was recorded in individual cells by imaging analysis system. Ratio imaging was obtained every 3 s, alternating excitation wavelengths at 490 nm and 405 nm, with the emission at 520 nm. In experiments aimed at evaluating the effect of Silybin on the basal activity of the NHE, HSC were acidified by adding 5 μ mol/L nigericin in nominally Na⁺/K⁺-free *N*-methyl-glucamine buffer. In this setting, a decrease in the fluorescence ratio indicates a decrease in cytosolic pH. When the fluorescence ratio value had stabilized, the administration of 50 mmol/L of NaCl caused a rapid cytosolic alkalinization, indicating restored Na/H antiporter activity; the kinetic of alkalinization is an index of the NHE activity. EIPA, a NHE inhibitor, was used as control drug. Cells were pre-incubated with the drug to be tested 10 min before the acidification.

2.12. Measurement of MCP-1, IL-8, MMP-2 and pro-collagen Type I secretion

Confluent HSC in 24-well plates were deprived of serum for 24 h. After replacement with 500 μ l of fresh SFIF medium, cells were treated with different agonists at the indicated doses and time points. At the end of the incubation, conditioned medium was collected and stored at –20 °C until assayed. Monocyte chemoattractant protein-1 (MCP-1) concentration in the medium was measured by enzyme-linked immunosorbent assay (ELISA), using a commercially available antibody kit (Biosource, Camarillo, CA). Interleukin (IL)-8 was assayed using a commercially available sandwich ELISA (BLK Diagnostics, Barcelona, Spain). Matrix metalloproteinase-2 (MMP-2) concentration was measured by ELISA using a commercially available antibody kit (Calbiochem San Diego, CA). Pro-collagen type I was detected by Pro-collagen Type I C-peptide EIA kit (Takara Bio Inc).

2.13. Statistical analysis

Unless otherwise specified, results, relative to the number of experiments indicated, are expressed as means \pm SD. Statistical analysis was performed by one-way analysis of variance and, when the *F* value was significant, by Duncan's test.

3. Results

3.1. Silybin reduces PDGF-induced DNA synthesis and cell proliferation

The effect of increasing concentrations of Silybin on PDGF-BB-induced DNA synthesis, measured as

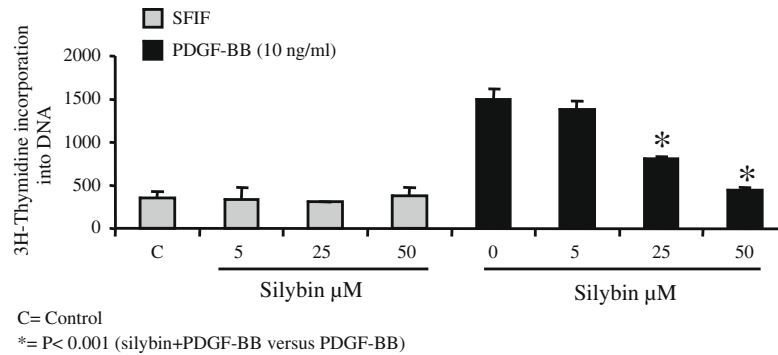


Fig. 1. Effect of Silybin on cell proliferation in activated human HSC. Dose–response for the effect of increasing concentrations of Silybin on PDGF-induced DNA synthesis, evaluated as [³H]TdR incorporation into DNA. Data are means ± SD for three experiments performed in triplicate. Compared with the effect of PDGF alone, changes were statistically significant starting at 25 μM of Silybin.

[³H]thymidine incorporation into DNA, was evaluated. As shown in Fig. 1, pre-incubation with Silybin for 5 min induced a dose-dependent inhibition of PDGF-induced mitogenesis. This inhibitory effect was statistically significant starting at 25 μM. Growth curves for activated human HSC in response to PDGF-BB with or without Silybin were analyzed to determine whether the decrease in PDGF-induced DNA synthesis was associated with an actual decrease in cell growth. As illustrated in Fig. 2, PDGF-BB at the dose of 10 ng/mL significantly increased HSC growth after 2, 4, and 6 days of incubation when compared with unstimulated control cells. This effect was clearly reduced by pre-treatment with Silybin, and this reduction was already statistically significant after 2 days of culture.

To exclude toxic effects of Silybin in these experimental conditions, different concentrations of Silybin were tested for cytotoxicity on cells maintained for 24 or 48 h in SFIF medium. No significant toxic effect was detected in the concentration range 5–100 μM (data not shown).

3.2. Silybin reduces PDGF-induced cell migration

To evaluate the effect of Silybin on cell motility, two different experimental approaches were used: the evaluation of chemotaxis in a modified Boyden chamber system and the wound-healing migration assay. As illustrated in Fig. 3, incubation of HSC with PDGF-BB for 6 h stimulated cell chemotaxis. In the presence of Silybin, this effect was reduced dose-dependently. Fig. 4 shows wounded monolayers incubated in medium containing PDGF-BB without or with increasing doses of Silybin. PDGF induced cell migration leading to wound closure 20 h after wounding. In the presence of Silybin, PDGF-induced cell migration in the wounded area was inhibited in a dose-dependent fashion.

3.3. Effect of Silybin on platelet-derived growth factor-induced intracellular signalling

To investigate the mechanisms responsible for the effect of Silybin on PDGF-induced cell proliferation

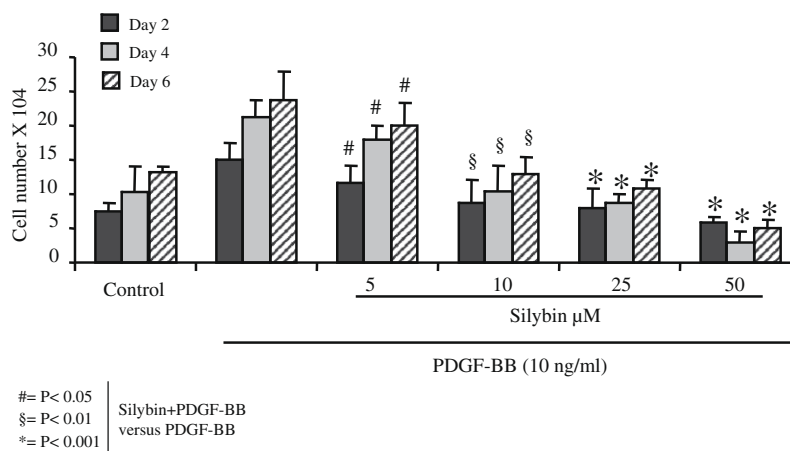


Fig. 2. Effect of Silybin on cell proliferation. HSC were plated on 12-well dishes; after 24 h, cells were washed with SFIF medium and incubated in fresh SFIF alone (control) or PDGF-BB (10 ng/mL) with or without increasing doses of Silybin. At each time point, cells were trypsinized and counted with a Burkert cell counter. Data are the mean values ± SD for two experiments performed in duplicate.

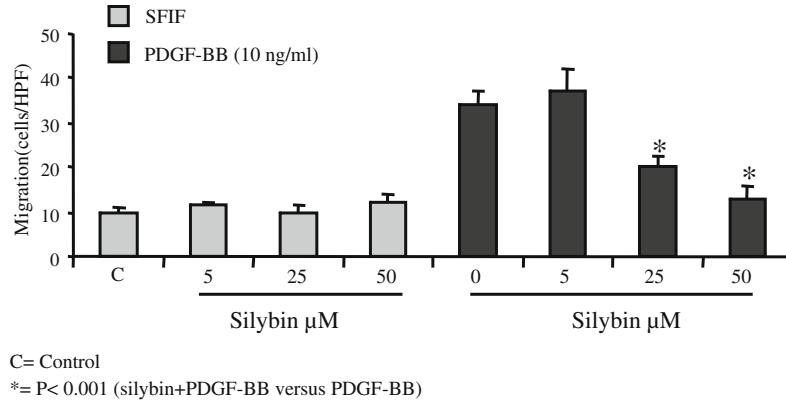


Fig. 3. Effect of Silybin on PDGF-induced chemotaxis in activated human HSC. Cell migration was determined in modified Boyden chambers as described in Materials and methods. Compared with the effect of PDGF alone, changes were statistically significant starting at 25 μM of Silybin. Data are means \pm SD for three experiments performed in triplicate. Compared with the effect of PDGF alone, changes were statistically significant starting at 25 μM of Silybin.

and migration, we first analyzed the effects of Silybin on PDGF-induced intracellular signalling. HSC were pretreated for 5 min with increasing concentrations of Silybin and then exposed to PDGF-BB (10 ng/mL) for 10 min. As shown in Fig. 5, in the absence of Silybin, PDGF induced a marked increase in ERK, MEK, Raf, and Akt phosphorylation. Silybin, at any concentration used, inhibited ERK, MEK, and Raf phosphorylation, but had no effect on Akt phosphorylation.

3.4. Effects of Silybin on the *de novo* synthesis of collagen type I and MMP-2

In this set of experiments, additional potential anti-fibrogenic properties of Silybin were evaluated, particularly the effect of this drug on TGF- β induced *de novo* synthesis of collagen type I, the major fibrillar ECM component. Pre-treatment with 25–50 μM Silybin significantly reduced TGF- β induced *de novo* synthesis of pro-collagen type I in cell supernatants (Fig. 6). As shown in

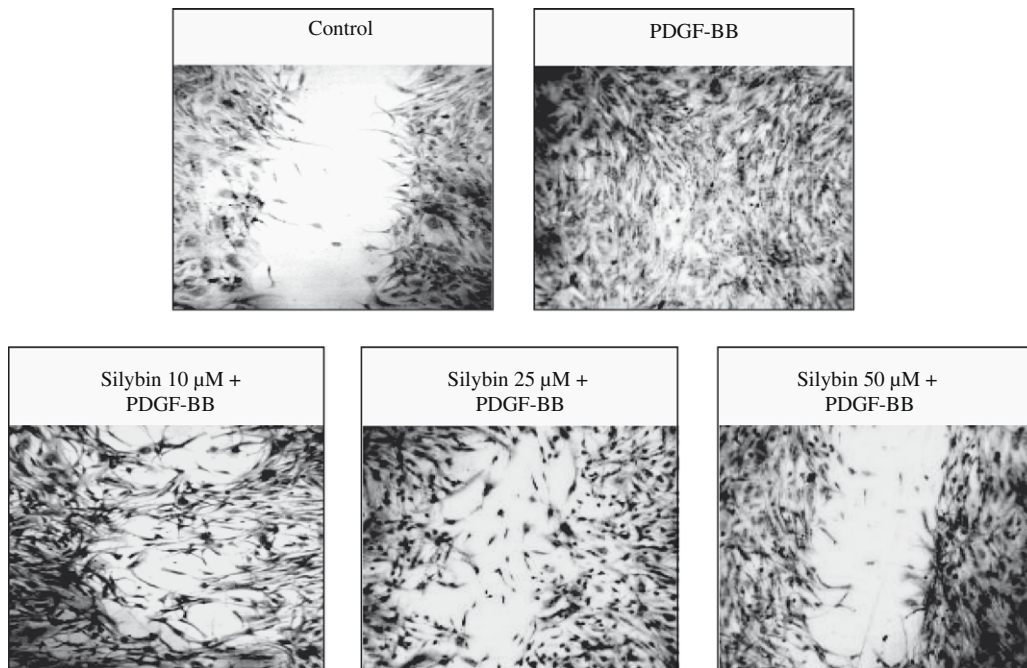


Fig. 4. Wound-healing assay. Confluent cell cultures were incubated in serum-free/insulin-free (SFIF) medium for 48 h before the beginning of the experiment. Monolayers were then disrupted to generate a linear wound with a cell scraper of approximately 1 mm, washed to remove debris, and incubated in medium containing PDGF-BB (10 ng/mL) in the presence or absence of increasing doses of Silybin for 20 h. Monolayers were then fixed and photographed by phase contrast microscopy. Experiments were performed in duplicate and 2 fields of each well were recorded.

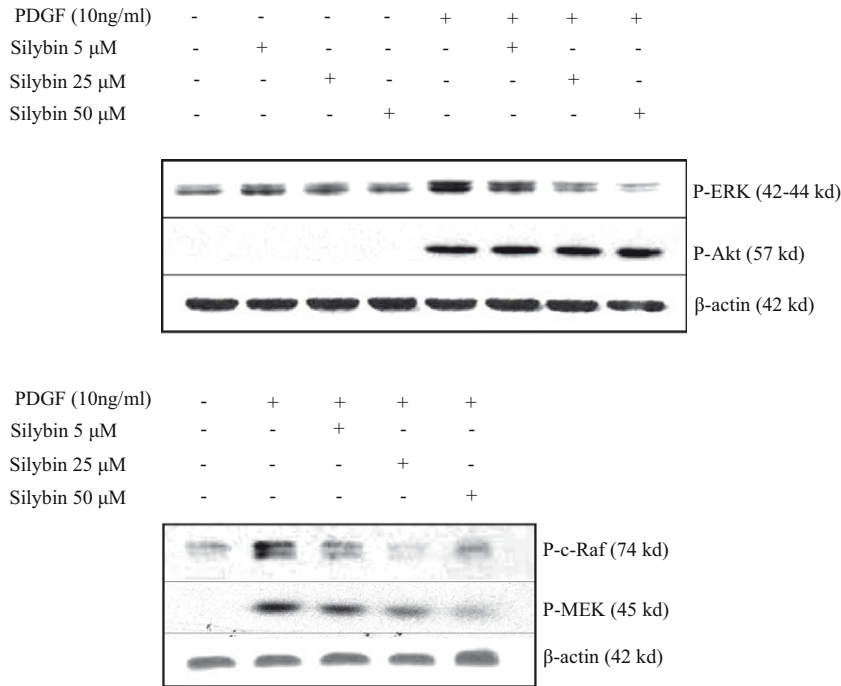


Fig. 5. Effect of Silybin on platelet-derived growth factor-induced intracellular signalling. Serum-deprived HSC were exposed to 5–50 μM of Silybin and then exposed to PDGF-BB (10 ng/mL) for 10 min. Representative Western blot results of P-ERK, P-Akt, P-Raf, P-Mek. All gels are representative of at least two independent experiments.

Fig. 7, incubation with TGF-β stimulated the *de novo* synthesis of MMP-2, gelatinase, involved in the degradation of the normal ECM during active fibrogenesis. Co-incubation with three doses of Silybin did not affect TGF-β-induced MMP-2 levels in cell supernatants.

3.5. Effect of Silybin on intracellular pH and Ca²⁺ concentration

It has been shown that PDGF signalling involves changes in [Ca²⁺]_i and [pH]_i in HSC. We investigated whether Silybin could modulate these changes. We first evaluated the effect of Silybin on the basal activity of the

Na⁺/H⁺ exchanger (NHE) that regulates [pH]_i in HSC. As illustrated in Fig. 8, untreated cells (control) recovered readily from a nigericin-induced acid load. The activity of the NHE was blocked completely by EIPA (ethylisopropylamiloride), an established Na⁺/H⁺ antiporter inhibitor employed as positive control. Changes in basal Na⁺/H⁺ antiporter activity were statistically significant when Silybin was used at 25–50 μM. We next evaluated the effect of Silybin on the changes in [Ca²⁺]_i. As previously shown, treatment with PDGF induced in

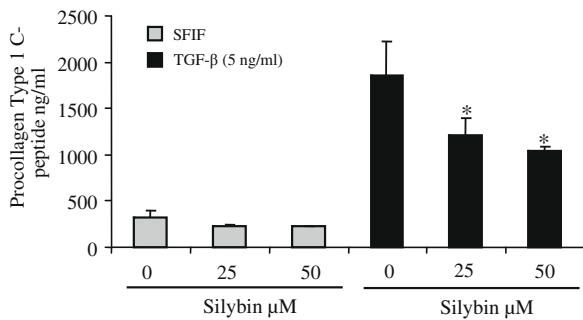


Fig. 6. Effect of Silybin on the *de novo* synthesis of pro-collagen type I. The *de novo* synthesis of pro-collagen type I by activated human HSC was determined in human HSC supernatants by ELISA as described in Materials and methods. Data are the mean values ± SD for three experiments performed in triplicate.

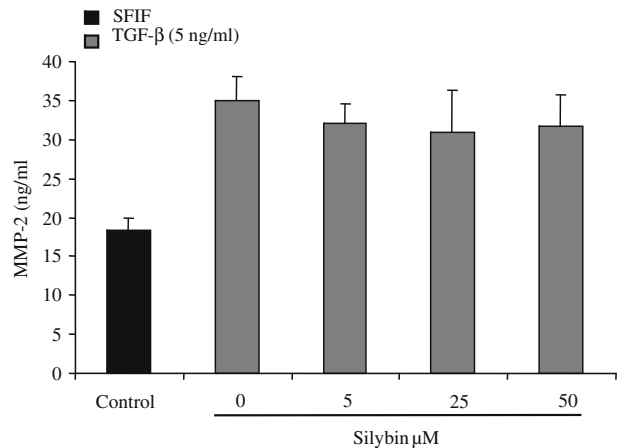


Fig. 7. Effect of Silybin on TGF-β-induced *de novo* synthesis of MMP-2. The *de novo* synthesis of MMP-2 by activated human HSC was determined in human HSC supernatants by ELISA as described in Materials and methods. Data are the mean values ± SD for two experiments performed in triplicate.

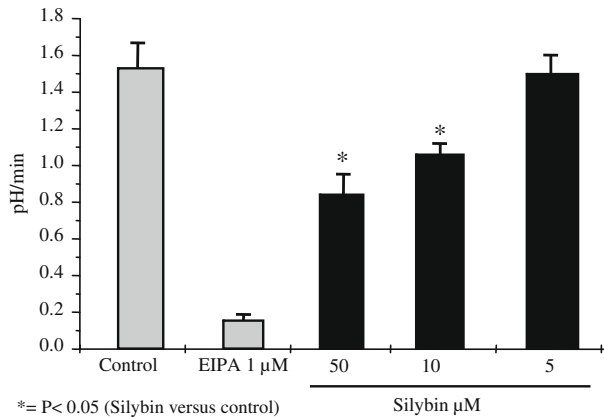


Fig. 8. Effect of Silybin on basal Na^+/H^+ exchanger activity (pH recovery after nigericin-induced acid load). Human HSC were loaded with 2 mol/L of bis-carboxyethylcarboxyfluorescein (BCECF) for 30 min and fluorescence was recorded in individual cells by imaging analysis system as described in material and methods. Changes in basal Na^+/H^+ antiporter activity were statistically significant when Silybin was used at 10–50 μM . The Na^+/H^+ antiporter inhibitor EIPA (10 $\mu\text{mol/L}$) was used as positive control.

HSC an increase in $[\text{Ca}^{2+}]_i$ that was characterized by a peak phase, followed by a long-lasting plateau (Fig. 9). Silybin did not inhibit either the peak increase or the plateau phase at any of the concentrations tested.

3.6. Effects of Silybin on IL-1 β -induced pro-inflammatory chemokines and cytokines

To investigate the role of Silybin in modulating the pro-inflammatory properties of HSC, cells were stimulated with IL-1 β (20 ng/ml), a potent pro-inflammatory cytokine. Silybin inhibited, in dose-dependent manner, IL-1-induced synthesis of human MCP-1 (monocyte chemoattractant protein 1) and human IL-8 as detected in cell supernatants (Fig. 10). Of note, treatment of cell

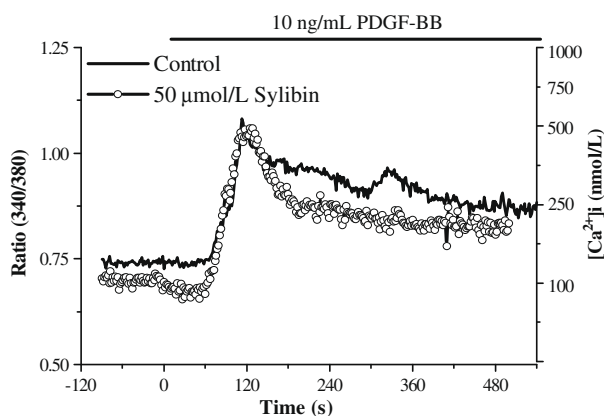


Fig. 9. Effect of Silybin on $[\text{Ca}^{2+}]_i$. Subconfluent HSC were maintained in SFIF for 48 h and were then loaded with Fura 2-AM to evaluate $[\text{Ca}^{2+}]_i$, as described in Materials and methods. Measurement were obtained in individual cells at 3-s time intervals.

cultures with Silybin also affected the basal synthesis of human MCP-1.

3.7. Effect of Silybin on IL-1 β -induced I κ -B α phosphorylation

To investigate the mechanisms responsible for the effect of Silybin on IL-1 β -induced synthesis of human MCP-1 and human IL-8, we analyzed the effects of Silybin on IL-1 β -induced I κ -B α phosphorylation. HSC were pre-treated for 5 min with increasing concentrations of Silybin and then exposed to IL-1 β (20 ng/mL) for 30 min. As shown in Fig. 11, in the absence of Silybin, IL-1 β -induced a marked increase in I κ -B α phosphorylation. Silybin completely inhibited this effect at any concentration used.

3.8. Effect of Silybin on intracellular ROS generation

The intracellular generation of ROS detected by using the conversion of 2',7'-dichlorodihydrofluorescein diacetate (DCFH-DA) in response to three different sets of pro-oxidant stimuli, i.e. hydrogen peroxide, X/XO and DMNQ was evaluated in the presence or absence of 50 μM Silybin. As summarized in the barogram (Fig. 12), Silybin at the concentration tested was able to markedly reduce the generation of intracellular ROS induced by the three standard pro-oxidizing systems.

4. Discussion

Silybin, a flavolignane isolated from the fruits of milk thistle, *S. marianum* has been shown to have hepatoprotective and anti-fibrotic properties in CLD. However, in spite of its global use, the molecular mechanisms responsible for the potential therapeutic effects of Silybin are still not fully elucidated.

In this study, performed in an established *in vitro* model of human hepatic fibrogenesis, Silybin demonstrated both direct and indirect anti-fibrotic properties by reducing PDGF-induced cell proliferation and migration, and by reducing TGF- β induced *de novo* synthesis of collagen type I, respectively. Furthermore, Silybin inhibited the IL-1-induced synthesis of human MCP-1 and human IL-8 in a dose-dependent manner, thus indicating a potentially relevant anti-inflammatory activity. Along these lines, MCP-1 expression is directly related to the number of monocytes infiltrating the portal tract during chronic hepatitis and is implicated as mediator in non-alcoholic steatohepatitis (NASH) and in insulin resistance [26,27]. In addition, MCP-1 secretion by HSC may contribute not only to the recruitment, but also to the activation of freshly recruited monocytes at the site of injury. IL-8, another chemokine secreted by

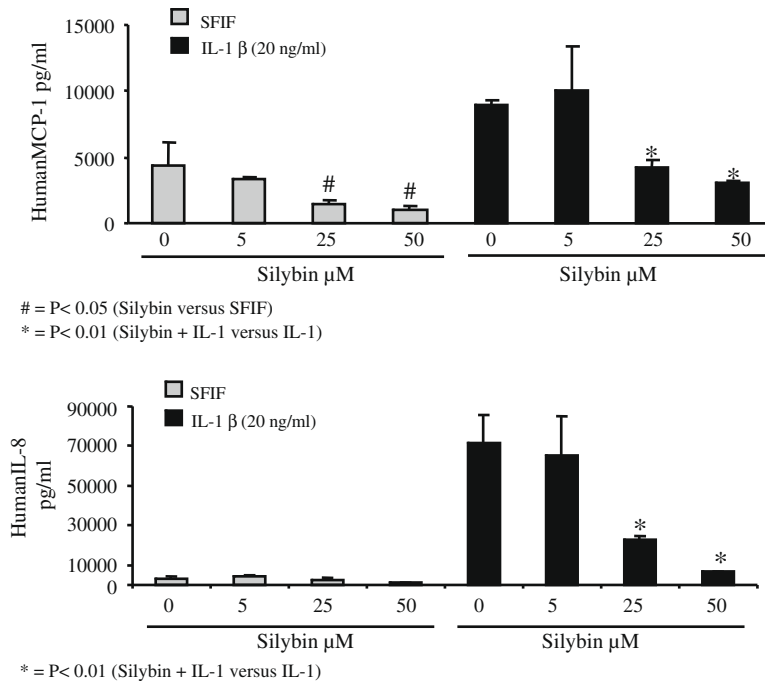


Fig. 10. Effect of Silybin on IL-1-induced *de novo* synthesis of MCP-1 and IL-8. IL-1-induced *de novo* synthesis of MCP-1 and IL-8 by activated human HSC determined in human HSC supernatants by ELISA as described in Materials and methods. Data are the mean values ± SD for three experiments performed in triplicate. No significant difference in total protein concentration/well was detected for each concentration of Silybin employed.

HSC is a potent chemoattractant activity for neutrophils and is a critical mediator of intrahepatic leukocyte recruitment [28].

To elucidate the molecular mechanisms responsible for the inhibition of PDGF-induced cell proliferation and migration, specific experiments were designed to detect the effect of Silybin on the PDGF signalling cascade. Pre-incubation with Silybin affected early signalling events associated with the PDGF receptor activation, including ERK, MEK, and c-Raf phosphorylation, involved in HSC proliferation, migration and collagen deposition.

Because PDGF signalling also involves changes in [Ca²⁺]_i and [pH]_i, we next investigated whether Silybin could modulate these events. Intracellular levels of H⁺ are regulated by the NHE, together with other antiporters (HCO₃⁻/Cl⁻, Na⁺/K⁺ adenosine triphosphatase).

In addition, its activity is stimulated by several agonists, including growth factors such as PDGF, as also reported in human HSC [4,29]. Our results indicate that Silybin is able to inhibit the antiporter activity in a dose-dependent fashion. Studies performed on different cell types have shown that activation of the NHE is dependent on the activation of different intracellular signalling pathways, including the Ras-mediated ERK cascade. In keeping with this observation, the effect of Silybin on NHE activity could be ascribed to the observed inhibitory action on ERK, MEK, and Raf activity.

Active NF-kappaB is involved in the transcriptional regulation of MCP-1 and IL-8 genes following stimulation with IL-1. Therefore we investigated whether or not Silybin is able to affect the activation of this transcriptional regulator. The NF-kappaB transcription factor is present in the cytosol in an inactive state complexed with the inhibitory IkappaB proteins. Activation occurs via phosphorylation of IkappaB-alpha followed by proteasome-mediated degradation, resulting in the release and nuclear translocation of active NF-kappaB. IkappaB-alpha phosphorylation is activated by diverse extracellular signals including inflammatory cytokines, growth factors and chemokines. Because phosphorylation of IkappaB-alpha is essential for release of active NF-kappaB, phosphorylation of this molecule represents an excellent marker of NF-kappaB activation. In our study, in the absence of Silybin, IL-1β induced a marked increase in Ik-Bα phosphorylation, while pre-incubation with Silybin, at any concentration used,

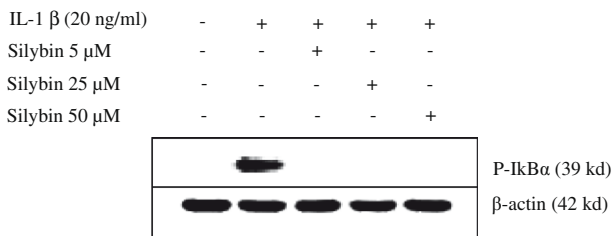


Fig. 11. Effect of Silybin on IL-1 β-induced intracellular signalling. Serum-deprived HSC were exposed to 5–50 μM of Silybin and then exposed to IL-1 β (20 ng/ml) for 30 min. Representative Western blot results of P-IkBα.

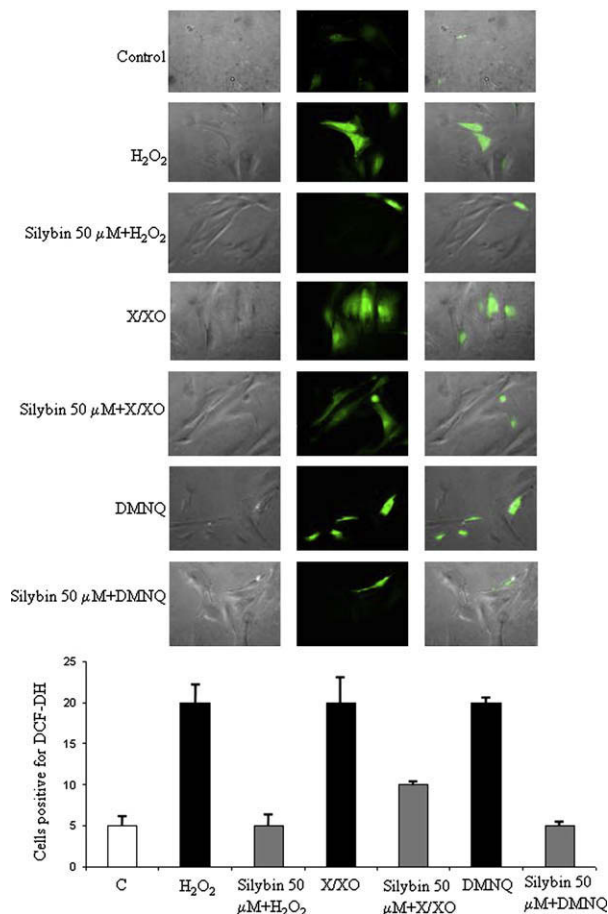


Fig. 12. Effect of Silybin (50 μ M) on intracellular ROS generation in response to three different sets of pro-oxidant stimuli, i.e. hydrogen peroxide, X/XO and DMNQ detected by using the conversion of 2',7'-dichlorodihydrofluorescein diacetate (DCFH-DA). The barogram summarizes the results derived from the observation of ten different microscopic fields for each of two independent experiments. Data are the mean values \pm SD. * $P < 0.05$ or higher degree of significance. [This figure appears in colour on the web.]

completely inhibited this effect. This piece of evidence suggests that Silybin is potentially capable of counteracting intracellular signalling leading to the amplification of inflammation typical of activated HSC.

Silymarin is characterized by a well established anti-oxidant action [8], and this property has been recently confirmed for Silybin [30]. The results of our study indicate that Silybin is able to dramatically reduce the generation of intracellular ROS in response to different pro-oxidant stimuli. This finding raises several considerations in the interpretation of the results. Firstly, it is known that, independently of extracellular pro-oxidant stimuli, generation of intracellular ROS is part of PDGF intracellular signalling [31,32] leading to its biologic effects. In addition, an increase in intracellular ROS generation is associated with direct pro-fibrogenic effects, i.e. increased expression and secretion of pro-collagen type I [33], and with a defined pro-inflammatory action, i.e. increased expression and secretion of MCP-1 [34]. In

this context, it appears relevant that Silybin has been shown to exert potential therapeutic actions on other liver cells, including Kupffer cells, endothelial cells and hepatocytes [35–37].

Taken together these considerations lead to the conclusion that the main therapeutic actions of Silybin in conditions of chronic liver damage/inflammation/fibrogenesis are likely to be ascribed to its anti-inflammatory and anti-oxidant activity in a context characterized by reduced non-parenchymal cell activation and hepatoprotection.

From a practical point of view, it is important to stress that the effects of Silybin reported in the present study were obtained in the dose range 5–50 μ M, compatible with the serum concentrations of the drug observed after oral administration [38–40]. This information supports the results obtained in animal models and provides the basis for further development of both Silybin derivatives and Silybin conjugates, whose hepatic pharmacokinetics have been already delineated [38,41].

Acknowledgements

Marco Trappoliere was a recipient of a research prize from the Italian Society of Gastroenterology (SIGE). Monika Schmid was a recipient of a Sheila Sherlock Research Fellowship from the European Association for the Study of the Liver (EASL).

References

- [1] Parola M, Marra F, Pinzani M. Myofibroblast-like cells and liver fibrogenesis: emerging concepts in a rapidly moving scenario. *Mol Aspects Med* 2008;29:58–66.
- [2] Friedman SL. Hepatic stellate cells: protean, multifunctional, and enigmatic cells of the liver. *Physiol Rev* 2008;88:125–172.
- [3] Guimarães EL, Franceschi MF, Grivicich I, Dal-Pizzol F, Moreira JC, Guaragna RM, et al. Relationship between oxidative stress levels and activation state on a hepatic stellate cell line. *Liver Int* 2006;26:477–485.
- [4] Di Sario A, Svegliati Baroni G, Bendia E, Ridolfi F, Saccomanno S, Ugili L, et al. Intracellular pH regulation and Na⁺/H⁺ exchange activity in human hepatic stellate cells: effect of platelet-derived growth factor, insulin-like growth factor 1 and insulin. *J Hepatol* 2001;34:378–385.
- [5] Aleffi S, Petrai I, Bertolani C, Parola M, Colombatto S, Novo E, et al. Upregulation of proinflammatory and proangiogenic cytokines by leptin in human hepatic stellate cells. *Hepatology* 2005;42:1339–1348.
- [6] Tsuruta S, Nakamuta M, Enjoji M, Kotoh K, Hiasa K, Egashira K, et al. Anti-monocyte chemoattractant protein-1 gene therapy prevents dimethylnitrosamine-induced hepatic fibrosis in rats. *Int J Mol Med* 2004;14:837–842.
- [7] Wen Z, Dumas TE, Schrieber SJ, Hawke RL, Fried MW, Smith PC. Pharmacokinetics and metabolic profile of free, conjugated, and total silymarin flavonolignans in human plasma after oral administration of milk thistle extract. *Drug Metab Dispos* 2008;36:65–72.

- [8] Gazák R, Walterová D, Kren V. Silybin and silymarin, new and emerging applications in medicine. *Curr Med Chem* 2007;14:315–338.
- [9] Schümann J, Prockl J, Kiemer AK, Vollmar AM, Bang R, Tieg G. Silibinin protects mice from T cell-dependent liver injury. *J Hepatol* 2003;39:333–340.
- [10] Singh RP, Gu M, Agarwal R. Silibinin inhibits colorectal cancer growth by inhibiting tumor cell proliferation and angiogenesis. *Cancer Res* 2008;68:2043–2050.
- [11] Raina K, Blouin MJ, Singh RP, Majeed N, Deep G, Varghese L, et al. Dietary feeding of silibinin inhibits prostate tumor growth and progression in transgenic adenocarcinoma of the mouse prostate model. *Cancer Res* 2007;67:11083–11091.
- [12] Roy S, Kaur M, Agarwal C, Tecklenburg M, Sclafani RA, Agarwal R. p21 and p27 induction by silibinin is essential for its cell cycle arrest effect in prostate carcinoma cells. *Mol Cancer Ther* 2007;6:2696–2707.
- [13] Katiyar SK, Roy AM, Baliga MS. Silymarin induces apoptosis primarily through a p53-dependent pathway involving Bcl-2/Bax, cytochrome *c* release, and caspase activation. *Mol Cancer Ther* 2005;4:207–216.
- [14] Polyak SJ, Morishima C, Shuhart MC, Wang CC, Liu Y, Lee DY. Inhibition of T-cell inflammatory cytokines, hepatocyte NF- κ B signaling, and HCV infection by standardized Silymarin. *Gastroenterology* 2007;132:1925–1936.
- [15] Ferenci P, TM Scherzer, Kerschner H, Rutter K, Beinhardt S, Hofer H, et al. Silibinin is a potent antiviral agent in patients with chronic hepatitis C not responding to pegylated interferon/ribavirin therapy. *Gastroenterology* 2008;135:1561–1567.
- [16] Jia JD, Bauer M, Cho JJ, Ruehl M, Milani S, Boigk G, et al. Antifibrotic effect of silymarin in rat secondary biliary fibrosis is mediated by downregulation of procollagen alpha1(I) and TIMP-1. *J Hepatol* 2001;35:392–398.
- [17] Di Sario A, Bendia E, Taffetani S, Omenetti A, Candelaresi C, Marziani M, et al. Hepatoprotective and antifibrotic effect of a new silybin-phosphatidylcholine–Vitamin E complex in rats. *Dig Liver Dis* 2005;37:869–876.
- [18] Boigk G, Stroedter L, Herbst H, Waldschmidt J, Riecken EO, Schuppan D. Silymarin retards collagen accumulation in early and advanced biliary fibrosis secondary to complete bile duct obliteration in rats. *Hepatology* 1997;26:643–649.
- [19] Fuchs EC, Weyhenmeyer R, Weiner OH. Effects of silibinin and of a synthetic analogue on isolated rat hepatic stellate cells and myofibroblasts. *Arzneimittelforschung* 1997;47:1383–1387.
- [20] Casini A, Pinzani M, Milani S, Grappone C, Galli G, Jezequel AM, et al. Regulation of extracellular matrix synthesis by transforming growth factor-beta1 in human fat-storing cells. *Gastroenterology* 1993;105:245–253.
- [21] Pinzani M, Failli P, Ruocco C, Casini A, Milani S, Baldi E, et al. Fat-storing cells as liver-specific pericytes: spatial dynamics of agonist-stimulated intracellular calcium transients. *J Clin Invest* 1992;90:642–646.
- [22] Pinzani M, Gesualdo L, Sabbah GM, Abboud HE. Effects of platelet-derived growth factor and other polypeptide mitogens on DNA synthesis and growth of cultured liver fat-storing cells. *J Clin Invest* 1989;84:1786–1793.
- [23] Marra F, Gentilini A, Pinzani M, Ghosh Choudhury G, Parola M, Herbst H, et al. Phosphatidylinositol 3-kinase is required for platelet-derived growth factor's action on hepatic stellate cells. *Gastroenterology* 1997;112:1297–1306.
- [24] Rezvani HR, Dedieu S, North S, Belloc F, Rossignol R, Letellier T, et al. Hypoxia inducible factor-1alpha, a key factor in the keratinocyte response to UVB exposure. *J Biol Chem* 2007;282:16413–16422.
- [25] Failli P, Ruocco C, De Franco R, Caligiuri A, Gentilini A, Giotti A, et al. The mitogenic effect of platelet-derived growth factor in human hepatic stellate cells requires calcium influx. *Am J Physiol* 1995;269:1133–1139.
- [26] Haukeland JW, Damås JK, Konopski Z, Loberg EM, Haaland T, Goverud I, et al. Systemic inflammation in nonalcoholic fatty liver disease is characterized by elevated levels of CCL2. *J Hepatol* 2006;44:1167–1174.
- [27] Westerbacka J, Cornér A, Kolak M, Makkonen J, Turpeinen U, Hamsten A, et al. Insulin regulation of MCP-1 in human adipose tissue of obese and lean women. *Am J Physiol Endocrinol Metab* 2008;294:E841–E845.
- [28] Pinzani M, Marra F. Cytokine receptors and signaling in hepatic stellate cells. *Semin Liver Dis* 2001;21:397–416.
- [29] Caligiuri A, De Franco RM, Romanelli RG, Gentilini A, Meucci M, Failli P, et al. Antifibrogenic effects of canrenone, an antialdosteronic drug, on human hepatic stellate cells. *Gastroenterology* 2003;124:504–520.
- [30] Trouillas P, Marsal P, Svobodová A, Vostálová J, Gazák R, Hrbác J, et al. Mechanism of the antioxidant action of silybin and 2,3-dehydrosilybin flavonolignans: a joint experimental and theoretical study. *J Phys Chem A* 2008;112:1054–1063.
- [31] Kreuzer J, Viedt C, Brandes RP, Seeger F, Rosenkranz AS, Sauer H, et al. Platelet-derived growth factor activates production of reactive oxygen species by NAD(P)H oxidase in smooth muscle cells through Gi1.2. *FASEB J* 2003;17:38–40.
- [32] Juarez JC, Manuia M, Burnett ME, Betancourt O, Boivin B, Shaw DE, et al. Superoxide dismutase 1 (SOD1) is essential for H₂O₂-mediated oxidation and inactivation of phosphatases in growth factor signaling. *Proc Natl Acad Sci USA* 2008;105:7147–7152.
- [33] Casini A, Ceni E, Salzano R, Biondi P, Parola M, Galli A, et al. Neutrophil-derived superoxide anion induces lipid peroxidation and stimulates collagen synthesis in human hepatic stellate cells: role of nitric oxide. *Hepatology* 1997;25:361–367.
- [34] Marra F, DeFranco R, Grappone C, Parola M, Milani S, Leonarduzzi G, et al. Expression of monocyte chemotactic protein-1 precedes monocyte recruitment in a rat model of acute liver injury, and is modulated by vitamin E. *J Investig Med* 1999;47:66–75.
- [35] Dehmlow C, Murawski N, de Groot H. Scavenging of reactive oxygen species and inhibition of arachidonic acid metabolism by silibinin in human cells. *Life Sci* 1996;58:1591–1600.
- [36] Dehmlow C, Erhard J, de Groot H. Inhibition of Kupffer cell functions as an explanation for the hepatoprotective properties of silibinin. *Hepatology* 1996;23:749–754.
- [37] Singh RP, Dhanalakshmi S, Agarwal C, Agarwal R. Silibinin strongly inhibits growth and survival of human endothelial cells via cell cycle arrest and downregulation of survivin, Akt and NF- κ B: implications for angioprevention and antiangiogenic therapy. *Oncogene* 2005;24:1188–1202.
- [38] Wen Z, Dumas TE, Schrieber SJ, Hawke RL, Fried MW, Smith PC. Pharmacokinetics and metabolic profile of free, conjugated, and total silymarin flavonolignans in human plasma after oral administration of milk thistle extract. *Drug Metab Dispos* 2008;36:65–72.
- [39] Carini R, Comoglio A, Albano E, Poli G. Lipid peroxidation and irreversible damage in the rat hepatocyte model. Protection by the silybin-phospholipid complex IdB 1016. *Biochem Pharmacol* 1992;43:2111–2115.
- [40] Comoglio A, Tomasi A, Malandrino S, Poli G, Albano E. Scavenging effect of silipide, a new silybin-phospholipid complex, on ethanol-derived free radicals. *Biochem Pharmacol* 1995;50:1313–1316.
- [41] Zhao J, Agarwal R. Tissue distribution of silibinin, the major active constituent of silymarin, in mice and its association with enhancement of phase II enzymes: implications in cancer chemoprevention. *Carcinogenesis* 1999;20:2101–2108.